Science of the Total Environment 648 (2019) 1–11

Contents lists available at ScienceDirect

Science of the Total Environment

journal homepage: www.elsevier.com/locate/scitotenv

# Predicting the impacts of climate change, soils and vegetation types on the geographic distribution of *Polyporus umbellatus* in China

Yanlong Guo [a,b], Xin Li [b,c,d,*], Zefang Zhao [e], Zain Nawaz [a,b]

[a] Northwest Institute of the Eco-Environment and Resources, Chinese Academy of Sciences, Lanzhou 730000, China
[b] University of the Chinese Academy of Sciences, Beijing 100049, China
[c] Institute of Tibetan Plateau Research, Chinese Academy of Sciences, Beijing 100101, China
[d] CAS Center for Excellence in Tibetan Plateau Earth Sciences, Chinese Academy of Sciences, Beijing 100101, China
[e] College of Tourism and Environment, Shaanxi Normal University, Xian 710119, China

## HIGHLIGHTS

- We built a comprehensive habitat suitability model for a medicinal fungus *Polyporus umbellatus*.
- We separate considers the climate, soil and vegetation environmental demands for fungus species.
- In northeastern and southwestern China suitable habitats of *P. umbellatus* will continue spread.
- In central China, the original *P. umbellatus* production area will continue to decrease.
- Not have enough forestland is the main limiting factor, but the limiting effect of soil will increase.

## GRAPHICAL ABSTRACT

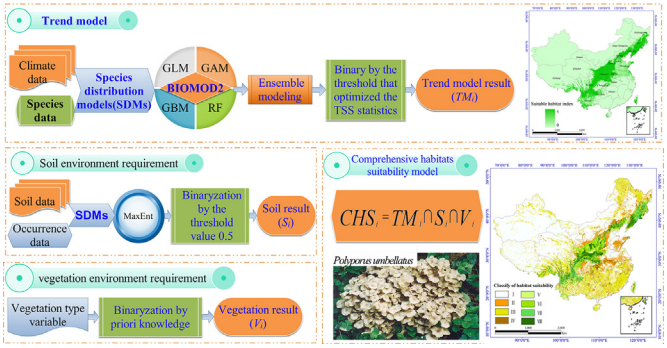


## ARTICLE INFO

*Article history:*
Received 11 February 2018
Received in revised form 31 July 2018
Accepted 31 July 2018
Available online 01 August 2018

Editor: Ouyang Wei

*Keywords:*
Geographic distribution
Medicinal fungus
*Polyporus umbellatus*
Species distribution models
MaxEnt

## ABSTRACT

*Polyporus umbellatus* is a fungus that has been used medically as a diuretic for thousands of years in China. To evaluate the impacts of climatic change on the distribution of *P. umbellatus*, we selected the annual mean air temperature, isothermality, minimum temperature of the coldest month, annual temperature range, annual precipitation and precipitation seasonality and used observations from the 2000s and simulated values from two future periods (2041 to 2060 and 2061 to 2080) to build an ensemble model (EM); then, we developed a comprehensive habitat suitability model by integrating soil and vegetation conditions into the EM to assess the distribution of suitable *P. umbellatus* habitats across China in the 2000s and the two future periods. Our results show that annual precipitation and annual mean air temperature together largely determine the distribution of *P. umbellatus* and those suitable *P. umbellatus* habitats generally occur in areas with an optimal annual precipitation of approximately 1000 mm and an optimal annual mean air temperature of approximately 13 °C. In other words, *P. umbellatus* requires a humid and cool environment for growth. In addition, brown soils with a granular structure and low acidity are more suitable for *P. umbellatus*. Furthermore, we have observed that the distribution of *P. umbellatus* is usually associated with the presence of coniferous, mixed coniferous, and broad-leaved forests,

*Abbreviations:* SDM, species distribution model; GLM, generalized linear model; GAM, generalized additive model; GBM, generalized boosting model; RF, random forest; MaxEnt, maximal entropy; PCA, principal component analysis; EM, ensemble model; TSS, true skill statistic; AUC, area under the receiver operating characteristic curve; CHS, comprehensive habitat suitability; Bio1, annual mean air temperature; Bio3, isothermality; Bio6, min temperature of the coldest month; Bio7, annual temperature range; Bio12, annual precipitation; Bio15, precipitation seasonality.

* Corresponding author at: 320 West Donggang Road, Northwest Institute of the Eco-Environment and Resources, Chinese Academy of Sciences, Lanzhou 730000, Gansu Province, China.
*E-mail addresses:* guoyl@lzb.ac.cn (Y. Guo), lixin@lzb.ac.cn (X. Li), lh_zzf.nn@snnu.edu.cn (Z. Zhao), zain-nawaz@lzb.ac.cn (Z. Nawaz).

https://doi.org/10.1016/j.scitotenv.2018.07.465

suggesting that these vegetation types are suitable habitats for *P. umbellatus*. In the future, annual precipitation and annual mean air temperature will continue to increase, consequently increasing the availability of habitats suitable for *P. umbellatus* in northeastern and southwestern China but likely leading to a degradation of suitable *P. umbellatus* habitats in central China.



## 1. Introduction

It is widely accepted that global climate changes will have significant effects on the natural distribution of species (Bertrand et al., 2011; Despland and Houle, 1997; Guo et al., 2017; Lenoir et al., 2008). Many studies have indicated that climate change is a significant driver of biodiversity loss, habitat fragmentation, and changes in the spatial patterns of species and can increase the risk of extinction for endangered species (Bálint et al., 2011; Boddy et al., 2014; Costion et al., 2015; Li et al., 2013). Detailed knowledge about the distribution of target species and their potential habitats is essential for rehabilitation (Adhikari et al., 2012; Lu et al., 2012). Moreover, understanding the impacts of climate change on species distribution has long-term implications for their protection and sustainable utilization (Forester et al., 2013; Summers et al., 2012). In recent decades, research concerns regarding the effects of climate change on species distribution have led to the widespread use of species distribution models (SDMs) (Anderson, 2013; Elith and Leathwick, 2009). However, due to the idiosyncratic life cycles and growth forms of fungi, few studies have focused on the distribution of fungi at large spatial and temporal scales (Guo et al., 2017; Suz et al., 2015; Yuan et al., 2015).

Medicinal fungi play an important role in healthcare and have been employed for millennia for the improvement of health and longevity (Phan et al., 2017). *Polyporus umbellatus*, a species of saprophytic fungus belonging to the Polyporaceae family, is one of the traditional Chinese medicinal fungi (He et al., 2017; Zhao, 2013). Sclerotia constitute the main component of *P. umbellatus* fungi and are commonly used to treat edema and promote diuretic processes (Bandara et al., 2015; Zhao, 2013). Modern pharmacology has confirmed that different compounds extracted from *P. umbellatus* have diuretic, anti-tumor, hepatoprotective, nephroprotective, and antioxidative properties (Bandara et al., 2015; He et al., 2017; Song et al., 2014; Zhao, 2013). Over the past two decades, the popularity of *P. umbellatus* in drug markets has increased due to its good clinical performance, which has led to shortages of this wild species (Xing et al., 2013). Climate change has impacted the environmental conditions in the original production area of *P. umbellatus*, which will increase the risk of resource shortages (Guo et al., 2017; Liu et al., 2015a; Tian, 2015; Zhang, 2014). Hence, the mapping of suitable *P. umbellatus* habitats and predictions of the impacts of climate change are vital for habitat protection and the sustainable development of this species.

SDMs have been widely employed to predict the potential distribution of species, particularly at large spatial and temporal scales (Anderson, 2013; Elith and Leathwick, 2009; Guo et al., 2017). SDMs relate species occurrence data to environmental predictor variables to simulate a species niche, and when combined with statistical or theoretical methods, SDMs can be used to map the potential distribution of species across landscapes and extrapolate these distribution over space and time (Elith and Leathwick, 2009; Guo et al., 2016). With technological advancements, numerous statistical methods and software applications have become widely available for describing patterns and performing predictions (Marmion et al., 2009; Naimi and Araújo, 2016; Zhao et al., 2017). Among these models, a generalized linear model (GLM) is a traditional regression algorithm that allows response variables to exhibit an error distribution other than a normal distribution. GLMs are common algorithms for SDMs (Guisan et al., 2002). Generalized additive models (GAMs) are semi-parametric extensions of GLMs that can address highly non-linear and non-monotonic relationships between a species distribution response and a set of explanatory environmental variables. GAMs are useful algorithms for species distribution research (Leathwick et al., 2006). Generalized boosting models (GBMs) combine the strengths of regression trees and boosting in an additive regression model in which the dividable terms are simple trees fitted in a forward, stage-wise manner (Moisen et al., 2006). Random forest (RF) algorithms are a common type of machine learning algorithm developed from classification and regression trees and bagging approaches. In species distribution research, the high precision of RF algorithms has been well established (Bradter et al., 2013; Mi et al., 2017). Maximal entropy (MaxEnt) models are currently the most popular SDMs because of various benefits such as being freely available and presenting a user-friendly operational interface (Merow et al., 2013; Phillips et al., 2006; Yuan et al., 2015). In addition, in MaxEnt models, both continuous and categorical data can be employed as environmental variable inputs (Guo et al., 2017; Merow et al., 2013). Various niche patterns cause differences in suitable habitat characteristics among species. The selection of optimal SDMs for particular species under designated space-time backgrounds is restricted by many factors, such as species niche characteristics, environment complexity, data availability, and data resolution. Hence, the ensemble model (EM) strategy, which combines the information from individual models fitted with different modeling techniques, has been proposed to solve this problem (Strubbe et al., 2015; Thuiller et al., 2009). Ensemble modeling avoids the selection of a single best model, thus eliminating (or at least limiting) model selection bias, but this approach also provides relative measures of the importance of each predictor across all candidate models (Burnham and Anderson, 2002; Guisan et al., 2017).

In this study, we collected species presence data from 80 locations and data on 32 environmental variables and used the EM strategy to simulate the migration trend of the *P. umbellatus* distribution under climate change scenarios. We then built a comprehensive habitat suitability model to predict the potential future geographic distribution of *P. umbellatus* in China. The objectives of this study were to predict the impacts of climate change on the potential habitats of *P. umbellatus* and to identify the key environmental variables limiting the distribution of *P. umbellatus*. This study provides an example of modeling the distribution of fungi and valuable insights for the protection of *P. umbellatus* resources.

## 2. Methods

### 2.1. Species occurrence data

*P. umbellatus* occurrence data were obtained from field survey reports from the last 10 years (Tian, 2015; Liu et al., 2015a; Xing et al., 2012; Liu et al., 2015b). Records with precise latitude and longitude information were selected to ensure geographic accuracy, and priority was given to records from the traditional *P. umbellatus* production area. Reasonable sampling sites were selected based on the following principles: First, only one record was retained for replicate site data, and based on the resolution of the environmental variables, we deleted some sampling points in the distribution point data aggregation area to ensure that the distance between two sampling points was always >10 km. Second, the sampling sites were selected based on different environmental conditions to ensure independence of the species

observations. Third, under the conditions for meeting the above two requirements, we deleted some sampling points to ensure that the points were distributed evenly. These operations allowed us to minimize the spatial autocorrelation of the sampling points and reduce its impact on the model's results. Finally, 150 records of species occurrence data were obtained for analysis (Fig. 1).

### 2.2. Environmental variables

The relevance and completeness of predictors are a key component in the building of SDMs (Elith and Leathwick, 2009; Guo et al., 2017; Zimmermann et al., 2010). In this study, we selected three types of environmental variables, including 19 bioclimatic variables and 13 soil and vegetation type variables (Table 1), and we resampled all of the variables at a 30″ (approximately 1 $km^2$) spatial resolution. Bioclimatic variables are assumed to be more biologically relevant than the original monthly climate layers from which the bioclimatic variables are derived; these variables are the most widely used climatic variables in SDMs. Future bioclimatic variable data for the 2050s and 2070s from four IPCC–CMIP5 (IPCC, 2013) representative concentration pathways (RCPs: RCP 8.5, RCP 6, RCP 4.5 and RCP 2.6) were downloaded from the International Center for Tropical Agriculture (http://ccafs-climate.org); these data were derived from three global climate models (GCMs) (CCSM4, MIROC5, and BCC–CSM1–1). Among the soil variables, the soil type (ST) variables were derived from the 1:1 million soil database of China, which was provided by the Data Center for Resources and Environmental Sciences, Chinese Academy of Sciences (RESDC). The other soil data were derived from the Harmonized World Soil Database (HWSD). The vegetation type variables were obtained from the 1:1 million China vegetation data set provided by the Environmental and Ecological Science Data Center for West China, National Natural Science Foundation of China (http://westdc.westgis.ac.cn).

### 2.3. Model evaluation

We constructed two models in this study, one for simulating the migration trend of the *P. umbellatus* distribution under climate change scenarios and the other for comprehensive prediction of the potential geographic distribution of *P. umbellatus* in the future considering limiting ecological factors. Because of the unique growth forms of fungal species, they do not grow in the absence of suitable vegetation and soil conditions, even if the climate and topography are favorable (Guo et al., 2017; Suz et al., 2015). Hence, in this study, we defined soil conditions and vegetation conditions as limiting ecological factors.

#### 2.3.1. Trend model

To reduce the uncertainty in the modeling results caused by different modeling techniques, we utilized the EM strategy to conduct the analysis. Here, we selected four different algorithms (GLM, GAM, GBM and RF) to build the EM. In addition, all model-building processes were conducted under the biomod2 framework. The modeling process was as follows (Fig. 2):

First, the bioclimatic variables were selected for the models. Previous studies have indicated that a serious multicollinearity problem exists among our 19 bioclimatic variables (Guisan et al., 2017; Yang et al., 2013); hence, we conducted a principal component analysis (PCA) to select a subset of the environmental variables (Guisan et al., 2017). In addition, according to the features of the distribution of the

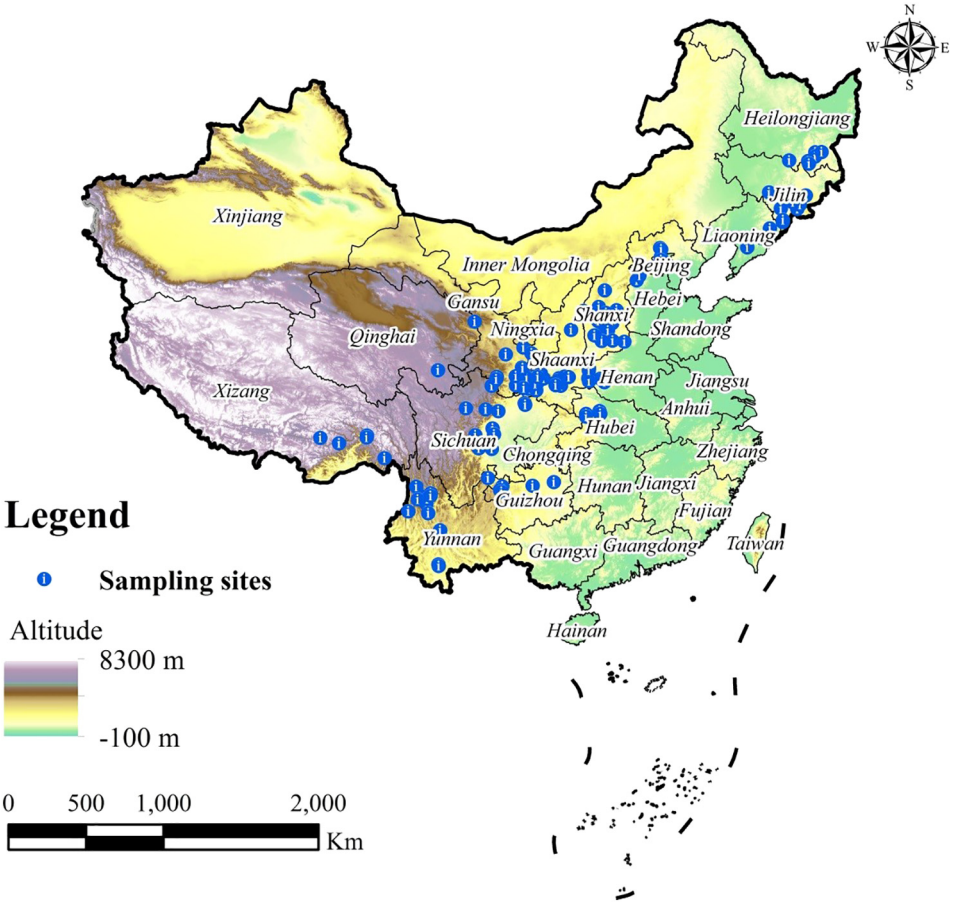


**Fig. 1.** Geographic locations of *Polyporus umbellatus* populations in China.

**Table 1**
Environmental variables used to predict the potential geographic distribution of *Polyporus umbellatus*.

| Classification and data source | Code | Description |
|---|---|---|
| Climatic variables | Bio1 | Annual mean air temperature |
| | Bio2 | Mean diurnal temperature range |
| | Bio3 | Isothermality |
| | Bio4 | Temperature seasonality |
| Data source | Bio5 | Max temperature of the warmest month |
| WorldClim database | Bio6 | Min temperature of the coldest month |
| (http://www.worldclim.org/) | Bio7 | Annual temperature range |
| | Bio8 | Mean temperature of the wettest quarter |
| | Bio9 | Mean temperature of the driest quarter |
| | Bio10 | Mean temperature of the warmest quarter |
| | Bio11 | Mean temperature of the coldest quarter |
| | Bio12 | Annual precipitation |
| | Bio13 | Precipitation of the wettest month |
| | Bio14 | Precipitation of the driest month |
| | Bio15 | Precipitation seasonality |
| | Bio16 | Precipitation of wettest quarter |
| | Bio17 | Precipitation of driest quarter |
| | Bio18 | Precipitation of the warmest quarter |
| | Bio19 | Precipitation of the coldest quarter |
| Soil variables | T_USDA | Topsoil USDA texture classification |
| | T_OC | Topsoil organic carbon (% weight) |
| Data source | T_PH | Topsoil pH ($H_2O$) |
| Harmonized World Soil Database (HWSD) (http://www.fao.org/soils-portal/) | T_CACO3 | Topsoil calcium carbonate (% weight) |
| Data Center for Resources and Environmental Sciences, | T_CASO4 | Topsoil gypsum (% weight) |
| Chinese Academy of Sciences (RESDC) (http://www.resdc.cn) | T_ESP | Topsoil sodicity (%) |
| | T_ECE | Topsoil salinity (dS/m) |
| | T_GRAVEL | Topsoil gravel content (% vol.) |
| | T_SAND | Topsoil sand fraction (% weight) |
| | T_SILT | Topsoil silt fraction (% weight) |
| | T_CLAY | Topsoil clay fraction (% weight) |
| | S_PH | Subsoil pH ($H_2O$) |
| | ST | Soil type variables |
| Vegetation variables | VT | 1:1 million China vegetation type data |
| Data source | | |
| Environmental and Ecological Science Data Center for West China, | | |
| National Natural Science Foundation of China (http://westdc.westgis.ac.cn) | | |

*P. umbellatus* occurrence data and the projection the 19 bioclimatic variables in the environmental space defined by the PCA (see Supplementary 1), we finally selected Bio1 (annual mean air temperature), Bio3 (isothermality), Bio6 (minimal temperature in the coldest month), Bio7 (annual temperature range), Bio12 (annual precipitation) and Bio15 (precipitation seasonality) as the modeling factors. In addition, we used the Pearson correlation coefficient (r) to examine the cross-correlation of these six variables, and the results showed that the correlation coefficients of these variables were <0.7.

Second, pseudo-absences were selected. We used random sampling methods to generate 500 pseudo-absence data points throughout the study area. To reduce the uncertainty of the random sampling, we repeated this process three times to generate a total of three datasets.

Third, single models were built. We ran four models separately on the biomod2 platform in the R software environment. All four models were evaluated using 80% of the data for model calibration and the remaining 20% for model testing. Furthermore, 10 replications were performed to reduce the uncertainty, and by default, each model was evaluated using the true skill statistic (TSS) and the values of the area under the receiver operating characteristic curve (AUC). Hence, in this step, we built a total of 120 single models (i.e., three pseudo-absence sampling models, four single modeling techniques, and 10 cross-validation runs).

Fourth, we generated the EM. For EM building, we chose the weighted average method to mix all single models with TSS values greater than or equal to 0.7 to produce our EMs. Thus, among the 120 single models built, only models with a TSS greater than or equal to 0.8 were retained to construct the final ensemble. We then utilized the TSS values to evaluate the references and thus determine the weights of the single model results. Eq. (1) illustrates how the TSS values were used to decide the weight of each single model:

$$w_j = \frac{r_j}{\sum_{j=1}^{h} r_j} \tag{1}$$

where $w_j$ is the weight of the model result $j$; $r_j$ is the TSS value of the model result $j$; and $h$ is the number of the model result. The normalization results of a single model were then multiplied by the corresponding weight to obtain the summation. Finally, we constructed the EM and calculated the potential habitat suitability index for *P. umbellatus* (Eq. (2)):

$$y_i = \sum_{j=1}^{n} w_j \times x_{ij} \tag{2}$$

where $y_i$ is the potential habitat suitability index of the first grid, $i$; $w_j$ is the weight of SDM $j$; $x_{ij}$ is the value of grid $i$ in the first SDM $j$; and $y_i$ (range [0,1]) is the evaluation index for the distribution of potentially suitable *P. umbellatus* habitats.

After the ensemble modeling was complete, we used the resulting model to study the potential distribution of *P. umbellatus* in the 2000s and under future conditions. The future climate change scenarios were defined by four RCPs (RCP 8.5, RCP 6.0, RCP 4.5 and RCP 2.6) and two periods (the 2050s and 2070s). The model was run separately for each period using future bioclimatic variable data (see Supplementary 2, Fig. S2). The future potential *P. umbellatus* distribution under each period was obtained by averaging the results.

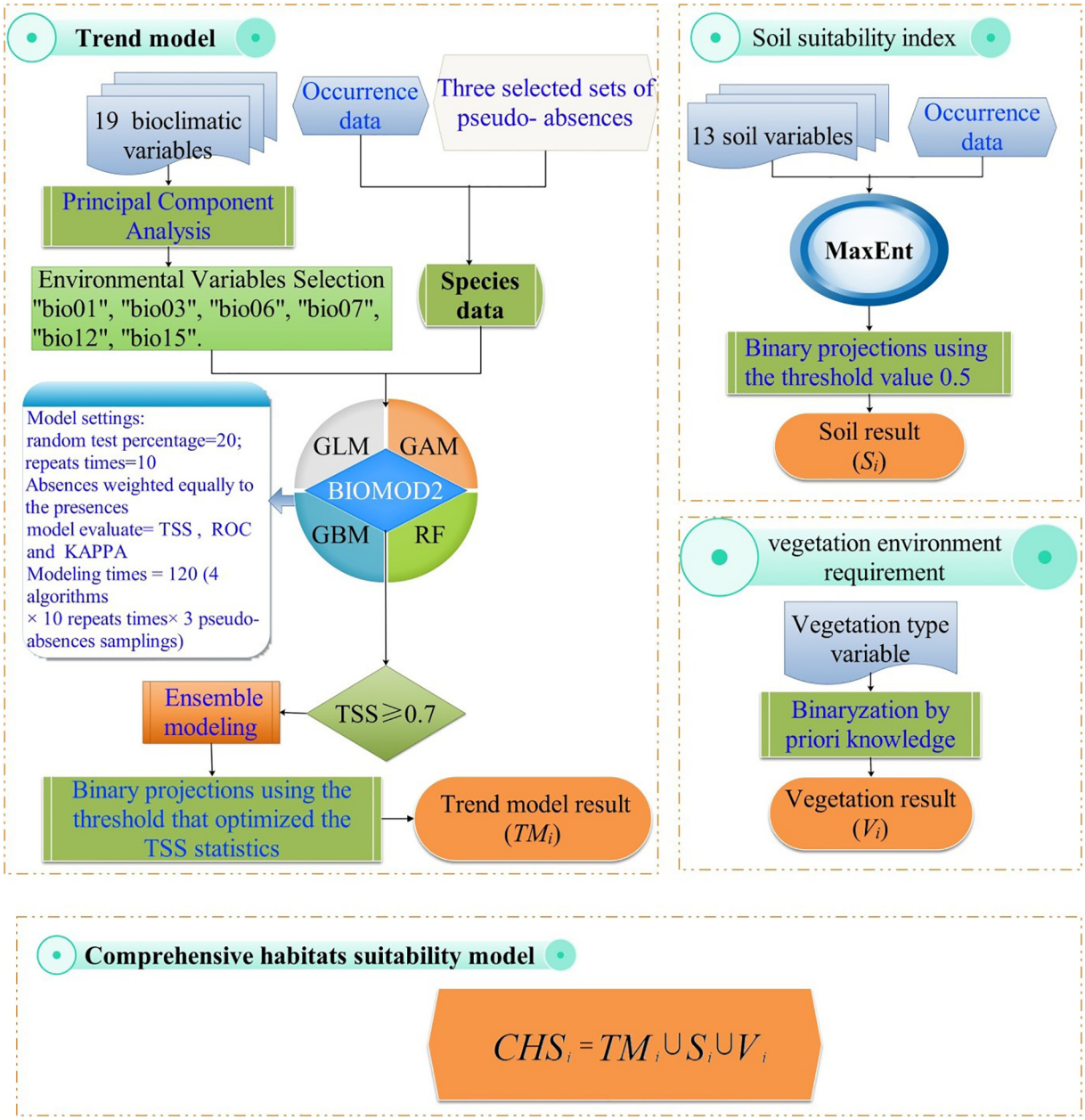


**Fig. 2.** Schematic representation of the methodological approaches.

Finally, the results of the ensemble modeling were projected in binary format. In this step, we used a threshold that optimized the TSS statistics from the testing data to transform the results of the EM (probability of occurrence) into binary projections (Guisan et al., 2017). TSS is a threshold-dependent metric, and a different threshold will result in different TSS values; here, we selected the threshold value corresponding to the maximal TSS value as the classification standard. Using the same threshold, the results for the 2000s and future trend models were reclassified into two categories: suitable and unsuitable.

*2.3.2. Binary projection of soil and vegetation conditions*

Soil type (ST) data provide information on important environmental factors that restrict the distributions of mushrooms; however, among the SDMs, only the MaxEnt model can use categorical data as environmental variable inputs. Hence, we employed the 13 soil variables and occurrence data for *N. incisum* to generate a MaxEnt model to determine soil environment requirements for the growth of *P. umbellatus*. The model was evaluated using 75% of the occurrence data for model calibration and 25% for model testing. Furthermore, 10 replications were performed to reduce the uncertainty, and the AUC was used to evaluate the model performance. The MaxEnt results for the soil environmental suitability index ranged from 0 to 1, and 0.5 was regarded as the threshold value for dividing the results into two categories: suitable (soil environmental suitability index ≥ 0.5) and unsuitable (soil environmental suitability index < 0.5).

Previous studies have precisely described the vegetation environment of *P. umbellatus*, which can grow naturally in both broad-leaved and coniferous forests (He et al., 2017; Li et al., 2012; Phan et al., 2017; Zhang, 2014; Zhao, 2013). Hence, we classified the vegetation type variable into two categories. The first category included coniferous, mixed coniferous, and broad-leaved forests, which were defined as suitable, whereas the second category included all other vegetation types, which were defined as unsuitable.

**Table 2**
The codes for the eight habitat suitability types.

| Code | Climate condition | Soil condition | Vegetation condition |
|---|---|---|---|
| I | Unsuitable | Unsuitable | Unsuitable |
| II | Unsuitable | Suitable | Unsuitable |
| III | Unsuitable | Unsuitable | Suitable |
| IV | Unsuitable | Suitable | Suitable |
| V | Suitable | Unsuitable | Unsuitable |
| VI | Suitable | Suitable | Unsuitable |
| VII | Suitable | Unsuitable | Suitable |
| VIII | Suitable | Suitable | Suitable |

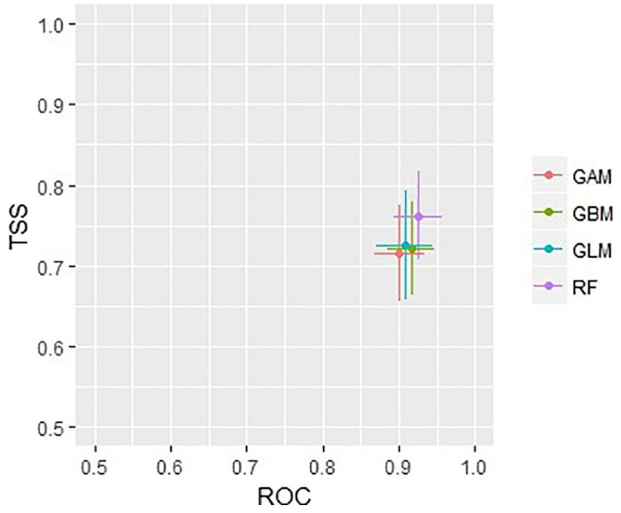


**Fig. 3.** Mean model evaluation scores according to two different evaluation metrics: the receiver operating characteristic (ROC) (AUC) and the true skill statistic (TSS). GAM: generalized additive model; GBM: generalized boosting models; GLM: generalized linear model; RF: random forest.

*2.3.3. Comprehensive habitat suitability (CHS) model*

Based on the trend model as well as comprehensive consideration of the restrictions on soil and vegetation conditions (Fig. 2), we built a CHS model to assess the distribution of suitable *P. umbellatus* habitats, and this model defined the CHS value in each evaluation unit (grid) for *P. umbellatus* as follows [Eq. (3)]:

$$CHS_i = TM_i \cap V_i \cap S_i \quad (3)$$

where $CHS_i$ represents the comprehensive habitat suitability conditions for *P. umbellatus* in each grid; $TM_i$ is the reclassified result of the trend model in three time periods (2000s, 2050s and 2070s) in each evaluation unit; $S_i$ is the result of the binary soil projection; and $V_i$ is the result of the binary vegetation projection. During the modeling process, the soil variables and vegetation type variables for the two future periods were assumed to remain unchanged. Therefore, we obtained eight different types of habitat suitability conditions for *P. umbellatus* for each time period (Table 2) and finally calculated the areas of all habitat suitability types.

## 3. Results

### 3.1. Model evaluation

According to the results of the model evaluation scores (Fig. 3), the TSS values of all models were >0.65, and the AUC values were >0.85; thus, nearly all calibrated models were satisfactory. However, in this study, only models with TSS values greater than or equal to 0.7 were retained to build the ensemble forecast. For the single models, all four algorithms were excellent and exhibited high evaluation scores: the average TSS values of all four algorithms were >0.7, and the AUC values were >0.88. Among the four algorithms, the RF models appeared to be the most accurate on average, followed by GLM, GBM and GAM (Fig. 2). Therefore, the EM (trend model) provided satisfactory results, with TSS and AUC values of 0.779 and 0.932, respectively. The soil environment requirement model also exhibited high accuracy, with an AUC value of 0.87; thus, the model results can be considered satisfactory.

### 3.2. Responses of the distribution of P umbellatus to environmental variables

SDMs can calculate the relative contributions of environmental variables to the distribution of a species. In this study, Bio12 (annual precipitation), Bio1 (annual mean air temperature), Bio7 (annual temperature range) and Bio6 (minimal temperature of the coldest month) made large contributions to the trend results obtained using all four algorithms. Among these four variables, Bio12 (annual precipitation) was the key factor determining the distribution of *P. umbellatus*. In addition, we defined the optimal and threshold values for these three environmental variables according to the response curves (Table 3). When the logistic probability of presence is maximal, the values of the environmental variables are optimal, and when the logistic probabilities of presence are >0.3, the range of the environmental variables is within the variable threshold (Table 3). Our model results indicated that the suitable range for Bio12 (annual precipitation) is approximately 600–1200 mm, and the optimal value is approximately 1000 mm. In addition, the suitable range and optimal value for Bio1 (annual mean air temperature) are approximately 5–17 °C and approximately 13 °C,

**Table 3**
Range, units, and optimal and threshold values for each key environmental variable.

| Environmental variables | Range and units | Optimal value | Suitable ranges |
|---|---|---|---|
| Bio12 | 12–5054 (mm) | 1000 | 600–1200 |
| Bio1 | −22.70-26.12 (°C) | 13.15 | 5.02–16.89 |
| Bio7 | 10.05–65.42 (°C) | 31.88 | 20.09–40.23 |
| Bio6 | −23.13–9.86 (°C) | −5.20 | −12.04–0.60 |
| ST | 12 orders, 61 suborders, and 227 groups. | Brown soil; white-starched brown soil | Yellow-brown soil; dark brown soil; yellow clunamon soil; brown calcareous soil; acidity skeleton soil; cinnamon soil; loess soil; albic soil; eluvial cinnamon soil |
| S_PH | 4.60–8.60 | 6.51 | 5.26–7.95 |
| T_ESP | 1–47 (%) | 1.03 | 0–5.42 |
| T_USDA | 9 types: clay (light); silty clay loam, clay loam, silt loam, loam; sandy clay loam; sandy loam; loamy sand, sand | Loamy sand | Silt loam, loam, sandy clay loam |
| T_GRAVEL | 0–32.00 (%) | 5.06 | >2.95% |
| TOC | 0–3.02 (%) | 1.50 | 1.20–2.43 |

Bio12: annual precipitation; Bio1: annual mean air temperature; Bio7: annual temperature range; Bio6: minimal temperature in the coldest month; ST: soil type variables; S_PH: subsoil pH ($H_2O$); T_ESP: topsoil sodicity; T_USDA: topsoil USDA texture classification; T_GRAVEL: topsoil gravel content; TOC: topsoil organic carbon.

respectively, and the optimal values for Bio7 (annual temperature range) and Bio6 (minimal temperature of the coldest month) are approximately 32 °C and approximately −5 °C, respectively (Table 3).

Regarding the soil suitability requirements of *P. umbellatus*, the MaxEnt results showed that ST (soil type variables), S_PH (subsoil pH), T_ESP (topsoil sodicity), T_USDA (topsoil USDA texture classification), T_GRAVEL (topsoil gravel content), and TOC (topsoil organic carbon) were the key soil factors determining the distribution of *P. umbellatus*. We defined the optimal and threshold values for the soil variables according to the response curves, for which the same criteria were employed (Table 3).

### 3.3. Trend of migration of the P. umbellatus distribution under climate change scenarios

The trend model results indicated that the main regions where *P. umbellatus* was distributed were located in the southwest, northeast and central regions of China. The distribution areas mainly covered the Changbai Mountain area located east of Heilongjiang, in Jilin and Liaoning Provinces; the northern parts of Hebei Province; parts of the Loess Plateau, including Shanxi, northern Shaanxi, and southern Gansu Provinces; the Qinling Mountains, including southern Shaanxi, Chongqing and western Hubei Provinces; the mountainous region in central Sichuan Province; parts of the Yunnan Guizhou Plateau; parts of the Hengduan Mountains located in southeastern Xizang Province; and a narrow region of east Shandong and Taiwan Provinces (Fig. 4).

By the 2050s, the *P. umbellatus* distribution areas will have markedly shifted toward the north in the Changbai Mountain area. Moreover, the distribution area will increase, particularly in the southeast of Heilongjiang Province, and new distribution areas will appear in Inner Mongolia Province, especially in the Da Hinggan Mountains. The distribution area will be drastically reduced in eastern Sichuan, Chongqing and western Guizhou Province. In addition, the trend of the northward movement of the distribution area will continue in the 2070s, and the distribution area will become fragmented due to distribution area losses in Yunnan, Guizhou, and central Shanxi Provinces. The new distribution area will be located mainly in the Da Hinggan Mountains (Fig. 4).

### 3.4. Suitable habitat distribution under global warming scenarios

The CHS model indicated that the suitable habitats of *P. umbellatus* in China decreased when the limiting ecological factors were considered. According to the area calculation results, the suitable habitat area for *P. umbellatus* (VIII type) in China was approximately $0.38 \times 10^6$ km$^2$; the area with suitable climate conditions, unsuitable soil conditions and suitable vegetation conditions (VII type) was approximately $0.23 \times 10^6$ km$^2$; and the area exhibiting suitable climate conditions, suitable soil conditions and unsuitable vegetation conditions (VI type) was approximately $0.40 \times 10^6$ km$^2$. The suitable habitats were mainly located in eastern Jilin Province, the Taihang Mountain area in the south of Shanxi Province, the Qinling Mountain area in southern Shaanxi Province, western Sichuan Province, central Henan Province, the Hengduan Mountains in southeastern Xizang Province and parts of northern Yunnan Province (Fig. 5). The largest amount of highly suitable habitats occurred in the Qinling Mountain area, which is generally considered a genuine production area.

By the 2050s, the model forecasts (Figs. 5 and 6) indicated that the suitable habitats for *P. umbellatus* will have shifted toward the north and slightly increased. New suitable habitats will occur in the northeast regions of China, mainly in eastern Heilongjiang Province. New suitable habitats will also occur in northern Hebei and northern Shanxi Provinces, and some small increases will occur in Yunnan and Xizang Provinces. In addition, losses and degradation of suitable habitats will mainly occur in the Qinling Mountains area, including western Hubei, Chongqing, and southern Shaanxi Provinces.

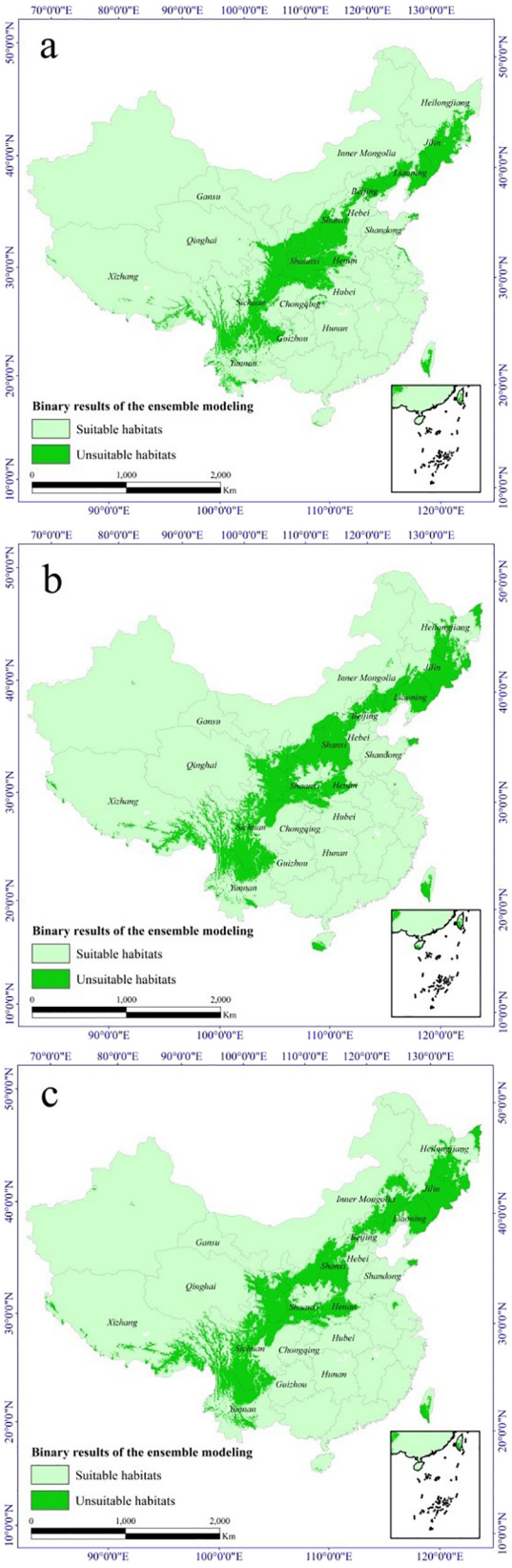


**Fig. 4.** Prediction of climatic habitat suitability for *Polyporus umbellatus* at different times in China. (a) 2000s, (b) 2050s, (c) 2070s.

The area of suitable *P. umbellatus* habitats will continue to shift toward the north and slightly decrease in the 2070s. Loss and degradation of suitable habitats will mainly occur in western Hubei and north-

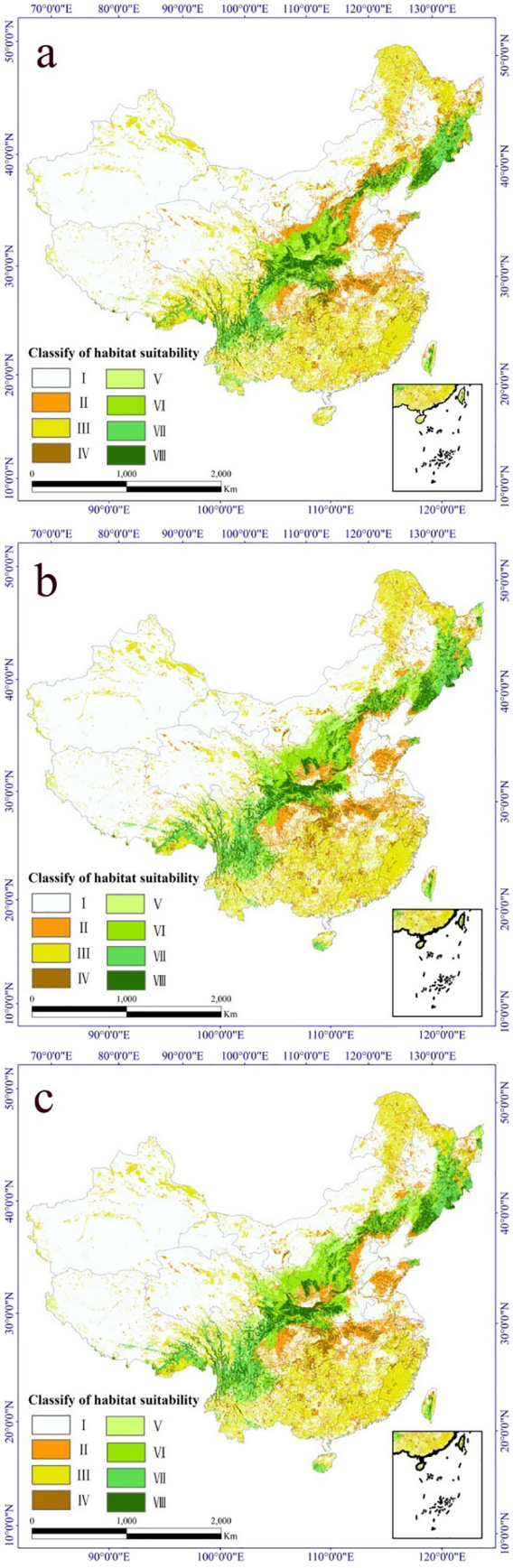


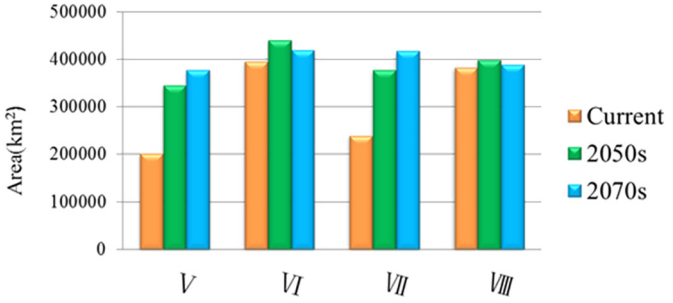


**Fig. 6.** Area of habitats of differing suitability for *Polyporus umbellatus* at different times in China. V: Habitat with suitable climate conditions and unsuitable vegetation and soil conditions; VI: Habitat with unsuitable vegetation conditions and suitable climate and soil conditions; VII: Habitat with unsuitable soil conditions and suitable climate and vegetation conditions; VIII: Suitable habitat.

central Shaanxi Provinces. In addition, new suitable habitats will mainly occur in eastern Heilongjiang Province in northeastern China, and the area of suitable habitats in Yunnan, Xizang and Sichuan Provinces will continue to increase.

## 4. Discussion

### 4.1. Ecological characteristics of P. umbellatus

Previous studies have yielded preliminary summaries of the ecological characteristics of *P. umbellatus* in China (Li et al., 2012; Zhang, 2014; Zhao, 2013). These studies have indicated that *P. umbellatus* exhibits a wide distribution in China, and the main production areas are located in Shaanxi, Yunnan, Shanxi, Henan, Gansu, Sichuan Provinces, among others, with Shaanxi Province presenting the richest reserves and best quality and Yunnan Province displaying the largest output. Based on the biological characteristics of *P. umbellatus* and phenological observations, we have a preliminary understanding of the mechanisms by which environmental factors affect its distribution. *P. umbellatus* is a middle-low temperature-adapted fungi. Mycelia of this fungus can grow at temperatures of 5–30 °C; when the temperature is above 30 °C or below 4 °C, the fungus stops growing and enters a natural dormancy stage. During the growth of *P. umbellatus* in the spring, when the temperature reaches 10 °C and the soil water content is 30%–50%, the sclerotia began to germinate. The mycelia break through the sclerotia epidermis and grow to form bacteria balls, subsequently becoming the white Ling (*P. umbellatus* with white coloration). In the summer, with the increase of temperature, the growth rate of white Ling is accelerated, and many new branches are formed. In the autumn, the temperature decreases, the growth of mycelia slows, and the color of the epidermis gradually deepens. In the winter, when the temperature decreases to 8–9 °C, *P. umbellatus* stops growth and enters hibernation. After overwintering, it becomes yellow or gray-yellow in color and is referred to as "gray Ling" (*P. umbellatus* with gray color). After another year of growth, *P. umbellatus* becomes black and is referred to as "black Ling" (*P. umbellatus* with black color). Only black Ling can be used as medicine (Li et al., 2012). The distribution areas of *P. umbellatus* exhibit some unique climatic characteristics, such as four

**Fig. 5.** Distribution of habitats of varying suitability for *Polyporus umbellatus* at different times in China. (a) 2000s, (b) 2050s, (c) 2070s. I: Unsuitable habitat; II: Habitat with suitable soil conditions and unsuitable climate and vegetation conditions; III: Habitat with suitable vegetation conditions and unsuitable climate and soil conditions; IV: Habitat with unsuitable climate conditions and suitable vegetation and soil conditions. V: Habitat with suitable climate conditions and unsuitable vegetation and soil conditions; VI: Habitat with unsuitable vegetation conditions and suitable climate and soil conditions; VII: Habitat with unsuitable soil conditions and suitable climate and vegetation conditions; VIII: Suitable habitat.

distinctive seasons and precipitation sufficient to maintain the soil water content at 30% to 50%. The annual precipitation in the distribution area of *P. umbellatus* is 500–1100 mm, and the annual average temperature is 4–18 °C (Li et al., 2012). It has been well documented that drought is unfavorable for the growth and development of *P. umbellatus*. The optimal growth temperature for *P. umbellatus* is 15 to 24 °C; its growth rate increases when the temperature is between 18 and 22 °C, and its growth is limited when the temperature is over 28 °C. Because *P. umbellatus* requires two growing seasons to reach the harvesting standard, winter temperature is another factor limiting the distribution of this species, as persistent low temperatures during the winter may lead to the death of underground sclerotia. Our model results indicated that the suitable range for Bio1 (annual mean air temperature) is 5–17 °C, and the optimal value is 13 °C. The suitable range for Bio12 (annual precipitation) is 600–1200 mm, and the optimal value is 1000 mm. In addition, the optimal values for Bio7 (annual temperature range) and Bio6 (minimal temperature of the coldest month) are 32 °C and −5 °C, respectively (Table 2). These data describe the climatic characteristics of temperate humid zones and subtropical humid zones, which are consistent with the biological characteristics of *P. umbellatus*.

Previous studies have shown that damp, porous loamy sand with rich humus is favorable for the growth of *P. umbellatus*, and the suitable range of the soil pH is 5.0–6.7 (Li et al., 2012; Xing et al., 2011). Our model results indicate that Brown soil and White-Starched Brown Soil are the most suitable for *P. umbellatus* growth, followed by Yellow-brown soil, Dark brown soil, Yellow clunamon soil, Brown calcareous soil, Acidity skeleton soil, Cinnamon soil, loess soil, Albic soil, Eluvial cinnamon soil. Regarding T_USDA (topsoil USDA texture classification), the optimal class is loamy sand. The optimal values for S_PH (subsoil pH ($H_2O$)), TOC (topsoil organic carbon) and T_GRAVEL (topsoil gravel content) are 6.5, 1.5% and 5, respectively (Table 2). These results clearly demonstrate the soil characteristics of suitable *P. umbellatus* habitats, i.e., low-acidity, porous soils with high carbon contents. In addition, the model results are consistent with the documentation. With respect to vegetation demands, for growth, *P. umbellatus* requires forestland with a high canopy density to provide humus for fungal growth and to preserve soil moisture; therefore, we selected coniferous, mixed coniferous, and broad-leaved forests as suitable vegetation types.

### 4.2. Characteristics of climate change in the main P. umbellatus distribution regions

To further elucidate how climate change affects the *P. umbellatus* distribution, we calculated the mean and standard deviation of the six bioclimatic variables included in the trend model for different climate scenarios and different time periods (Supplementary 2, Tables S1–4); these statistics were determined for four regions, including mainland China and three main *P. umbellatus* distribution regions (see Supplementary 2, Fig. S3). The results indicated that for mainland China, the average value of Bio1 (annual mean air temperature) in the 2000s was approximately 6.75 °C. In the future, under different IPCC climate change scenarios, Bio1 (annual mean air temperature) will show increasing trends, but the extent of increase will differ among scenarios. By the 2050s, the mean Bio1 (annual mean air temperature) value in mainland China may equal 8.80 °C, and by the 2070s, Bio1 (annual mean air temperature) may reach 9.25 °C; the corresponding increase in the temperature range will be 2.5 °C. Bio12 (annual precipitation) exhibits the same increasing trend: by the 2050s, the mean Bio12 (annual precipitation) value may increase by 27 mm, and by the 2070s, the increase will reach 44 mm. Bio3 (isothermality) and Bio15 (precipitation seasonality) will remain largely unchanged, showing only slight increases, and Bio7 (annual temperature range) will remain largely unchanged, showing a slight decrease. These findings indicate that the seasonal trends of temperature and precipitation will remain unchanged in mainland China. In contrast, Bio6 will increase significantly, likely by approximately 4 °C by the 2070s.

In southwest China, due to dramatic changes in elevation, a complicated topography and a variable climate, Bio12 (annual precipitation) and Bio1 (annual mean air temperature) vary widely in space, presenting high standard deviations. Thus, the *P. umbellatus* distribution areas present clear characteristics of habitat fragmentation, and the distribution is associated with altitude and moisture gradients. In the future, Bio12 (annual precipitation) and Bio1 (annual mean air temperature) will continue to increase; the mean Bio12 (annual precipitation) value will reach approximately 1000 mm by the 2070s, which is the optimal value for *P. umbellatus* distribution. Hence, suitable habitats for *P. umbellatus* will continue to spread in this area.

In northeastern China, because of the lower degree of land surface relief, Bio12 (annual precipitation) and Bio1 (annual mean air temperature) exhibit smaller degrees of change with smaller standard deviations, causing the *P. umbellatus* distribution regions to present the characteristics of an aggregating distribution. The main limiting climatic factor of the *P. umbellatus* distribution in this area is lower temperature; in the 2000s, the mean Bio1 (annual mean air temperature) and Bio6 (minimal temperature of the coldest month) values were 4.52 °C and −21.15 °C, respectively, and both of these values are below the lower limit of the suitable range. In the future, Bio12 (annual precipitation), Bio1 (annual mean air temperature) and Bio6 (minimal temperature of the coldest month) will continue to increase, and the ranges of increase will be significantly higher than the averages for mainland China. By the 2070s, Bio1 (annual mean air temperature) will increase to 7.58, reaching the suitable range for *P. umbellatus* distribution. Therefore, the suitable habitats for *P. umbellatus* will continue to expand and develop in this area.

In the central regions of China in the 2000s, Bio12 (annual precipitation) was 587 mm, which is below the lower limit of the suitable range. By the 2070s, Bio12 (annual precipitation) will increase to 605 mm, which represents an increase of only 18 mm (i.e., a smaller increase than the increases in northeastern and southwestern China). However, Bio1 (annual mean air temperature) in this region will increase significantly; by the 2070s, Bio1 (annual mean air temperature) will increase to 12.66 °C, which is 2.76 °C higher than the average temperature increase in mainland China. Additionally, the Bio15 value is lower in this region than in northeastern and southwestern China and will continue to decrease in the future, indicating that the seasonal variation of precipitation in this area will decrease in the future. In summary, insufficient precipitation is the main climatic factor limiting the *P. umbellatus* distribution in this area. With continuously increasing temperatures in the future, the growth of *P. umbellatus* will require more water, but the increase in precipitation will not reach the corresponding level. Additionally, less precipitation seasonality means less precipitation in the growing season. The combination of all these factors will cause continued decreases in the suitable habitats of *P. umbellatus* in this region.

### 4.3. Restrictive effects of soil and vegetation on suitable P. umbellatus habitats

Theoretically, *P. umbellatus* can shift its range to all areas where climate conditions are suitable, but as a wood-rotting fungus, unsuitable soil and vegetation conditions will limit the expansion of suitable habitats for this species. In addition, vegetation succession and the formation of suitable soil occur slowly in these areas under natural conditions, hindering the ability of fungal species to shift their ranges.

In the 2000s, under suitable climatic conditions, the area of unsuitable vegetation habitats (Fig. 6, V + VI) was larger than the area of unsuitable soil habitats (Fig. 6, V + VII). Therefore, vegetation conditions are currently the main factor limiting the distribution of this species. The distribution areas of unsuitable habitats (Fig. 6, V, VI, VII) around the three main regions of the *P. umbellatus* distribution present different features. Habitat type VII is widely distributed in southwest and

northeast China (Fig. 5), which demonstrates that the primary factor limiting the extension of the species distribution in these areas is unsuitable soil conditions. However, in the central region of China, especially in central Shaanxi Province, southern Shanxi Province and the Qinling Mountain area, habitat type VI is widely distributed (Fig. 5), which indicates that unsuitable vegetation is the main factor limiting the extension of the distribution of this species.

Our model forecast (Figs. 5 and 6) indicates that over time, the areas of habitat types V and VII will increase significantly (Fig. 6), which indicates that the limiting effect of soil conditions will gradually increase in the newly formed regions with a suitable climate for *P. umbellatus*. While the area of habitat type VII of *P. umbellatus* is relatively stable, this habitat type presented a trend of first increasing and then decreasing, with minor changes. The spatial distribution of unsuitable habitats (Fig. 5, V, VII, VIII) remains essentially unchanged. In addition, in southwest and northeast China, the distribution of habitat type VII will increase significantly. In central China, the range of habitat type VI will shift northward, whereas in the southern Qinling Mountains, central Shaanxi and northern Shanxi Provinces, habitat type VI will gradually decrease, and new areas of habitat type VI will occur to the north of Shaanxi and in northern Shaanxi, southern Gansu, and Ningxia Provinces.

### 4.4. SDMs for fungi

The distinctive lifecycles and growth forms of fungi pose enormous challenges for simulating the potential response of fungus distributions to climate change (Guo et al., 2017; Suz et al., 2015). Geographic information systems (GISs) and SDMs provide a possible solution to this problem. Because of the specific growth requirements of fungi, most fungal species (including *P. umbellatus*) require suitable host plants and soil environments. Hence, vegetation type and soil variables should be considered limiting factors during the modeling process (Guo et al., 2017). However, in the study of SDMs, researchers typically combine all environmental variables in one modeling strategy (Guisan et al., 2017; Li et al., 2013; Moisen et al., 2006; Yang et al., 2013; Zhao et al., 2017). Based on this modeling strategy, the model may not be able to distinguish between general environmental factors and limiting environmental factors; thus, SDMs for fungal species should be constructed separately for the climate, vegetation, and soil environments, and these can then by multiplied to calculate the CHS index for the entire study area. Thus, we can represent the limiting effects of vegetation factors and soil factors. Due to global warming, the suitable habitats for fungal species will theoretically shift to relatively higher altitudes and latitudes. However, under natural conditions, vegetation succession and the formation of particular STs are complex processes that generally take place over a long period, which will hinder the ability of fungal species to shift their distribution.

According to Suz et al. (2015), determining the key environmental factors that control the distribution of fungal species at landscape and larger scales has been one of the main directions of fungal research in the 2000s, and SDMs provide a practical method for addressing this issue. Based on authentic and appropriate amounts of species distribution records and reliable and sufficient environmental variables, SDMs can be employed to calculate the relative contributions of various environmental variables. Moreover, SDMs can quantify the relationship between environmental variables and habitat suitability (logistic probability of presence), and researchers can define the optimal and threshold values for fungal species according to these relationships. This information is essential for effective habitat protection and can also facilitate more effective plant cultivation.

## 5. Conclusions

We successfully built a CHS model that considers all climate, soil and vegetation environmental demands to identify suitable habitats for *P. umbellatus*. With this model, we examined the impacts of climate change on suitable *P. umbellatus* habitats in China. In contrast to common modeling strategies that combine all environmental variables into one modeling process, we defined the habitat requirements of vegetation and soil as limiting factors in our model according to the habitat characteristics of *P. umbellatus*. Our results suggest that climate change will significantly affect the distribution of suitable *P. umbellatus* habitats in the 2050s and 2070s and that its effects will vary among different regions. In northeastern China, due to rising temperature, particularly a rising minimal temperature in the coldest month, the suitable habitats for *P. umbellatus* will continue to increase and shift toward the north, and new suitable habitats for this medicinal fungus will develop in the Da Hinggan Mountains. In central China, due to gradual increases in air temperature and low precipitation during the growth period, the suitable habitats for *P. umbellatus* will continue to decrease and shift toward the north; some suitable habitats will be lost or will degrade. In southwest China, suitable habitats will extend to the interior of the plateau; simultaneously, new suitable habitats will occur in the central region of Yunnan Province, which will result in an increase in suitable habitats in this region. We believe our modeling approach can provide a clear understanding of the distribution of suitable habitats for a target species and identify the reasons why other areas are unsuitable, which can inform artificial cultivation and conservation efforts.

## Acknowledgements

### Funding

This study was financially supported by the Strategic Priority Research Program of the Chinese Academy of Sciences, Grant No. XDA19070100, the National Natural Science Foundation of China (Grant No. 91425303), and the 13th Five-year Informatization Plan of Chinese Academy of Sciences (Grant No. XXH13505-06).

### Competing financial interests

The authors have no conflicts of interest to declare.

## Appendix A. Supplementary data

Supplementary data to this article can be found online at https://doi.org/10.1016/j.scitotenv.2018.07.465.

## References

Adhikari, D., Barik, S.K., Upadhaya, K., 2012. Habitat distribution modelling for reintroduction of *Ilex khasiana*, purk. A critically endangered tree species of northeastern India. Ecol. Eng. 40, 37–43. https://doi.org/10.1016/j.ecoleng.2011.12.004.

Anderson, R.P., 2013. A framework for using niche models to estimate impacts of climate change on species distributions. Ann. N. Y. Acad. Sci. 1297, 8–28. https://doi.org/10.1111/nyas.12264.

Bálint, M., Domisch, S., Engelhardt, C.H.M., Haase, P., Lehrian, S., Sauer, J., Theissinger, K., Pauls, S.U., Nowak, C., 2011. Cryptic biodiversity loss linked to global climate change. Nat. Clim. Change 1, 313–318. https://doi.org/10.1038/nclimate1191.

Bandara, A.R., Rapior, S., Bhat, D.J., Kakumyan, P., Chamyuang, S., Xu, J., Hyde, K.D., 2015. *Polyporus umbellatus*, an edible-medicinal cultivated mushroom with multiple developed health-care products as food, medicine and cosmetics: a review. Cryptogam. Mycol. 36, 3–42. https://doi.org/10.7872/crym.v36.iss1.2015.3.

Bertrand, R., Lenoir, J., Piedallu, C., Riofrío-Dillon, G., de Ruffray, P., Vidal, C., Pierrat, J.C., Gégout, J.C., 2011. Changes in plant community composition lag behind climate warming in lowland forests. Nature 479, 517–520. https://doi.org/10.1038/nature10548 (Pubmed: 22012261).

Boddy, L., Büntgen, U., Egli, S., Gange, A.C., Heegaard, E., Kirk, P.M., Mohammad, A., Kauserud, H., 2014. Climate variation effects on fungal fruiting. Fungal Ecol. 10, 20–33. https://doi.org/10.1016/j.funeco.2013.10.006.

Bradter, U., Kunin, W.E., Altringham, J.D., Thom, T.J., Benton, T.G., 2013. Identifying appropriate spatial scales of predictors in species distribution models with the random forest algorithm. Methods Ecol. Evol. 4, 167–174. https://doi.org/10.1111/j.2041-210x.2012.00253.x.

Burnham, K.P., Anderson, D.R., 2002. Model Selection and Multimodel Inference: A Practical Information-Theoretic Approach. Springer, Berlin.

Costion, C.M., Simpson, L., Pert, P.L., Carlsen, M.M., John Kress, W.J., Crayn, D., 2015. Will tropical mountaintop plant species survive climate change? Identifying key knowledge gaps using species distribution modelling in Australia. Biol. Conserv. 191, 322–330. https://doi.org/10.1016/j.biocon.2015.07.022.

Despland, E., Houle, G., 1997. Climate influences on growth and reproduction of *Pinus banksiana* (Pinaceae) at the limit of the species distribution in Eastern North America. Am. J. Bot. 84, 928. https://doi.org/10.2307/2446283.

Elith, J., Leathwick, J.R., 2009. Species distribution models: ecological explanation and prediction across space and time. Annu. Rev. Ecol. Evol. Syst. 40, 677–697. https://doi.org/10.1146/annurev.ecolsys.110308.120159.

Forester, B.R., Dechaine, E.G., Bunn, A.G., 2013. Integrating ensemble species distribution modelling and statistical phylogeography to inform projections of climate change impacts on species distributions. Divers. Distrib. 19, 1480–1495. https://doi.org/10.1111/ddi.12098.

Guisan Jr., A., Edwards, T.C., Hastie, T., 2002. Generalized linear and generalized additive models in studies of species distributions: setting the scene. Ecol. Model. 157, 89–100. https://doi.org/10.1016/S0304-3800(02)00204-1.

Guisan, A., Thuiller, W., Zimmermann, N.E., 2017. Habitat Suitability and Distribution Models: With Applications in R. Cambridge University Press, Cambridge.

Guo, Y.L., Wei, H.Y., Lu, C.Y., Gao, B., Gu, W., 2016. Predictions of potential geographical distribution and quality of *Schisandra sphenanthera* under climate change. PeerJ 4, e2554. https://doi.org/10.7717/peerj.2554.

Guo, Y.L., Li, X., Zhao, Z.Z., Wei, H., Gao, B., Gu, W., 2017. Prediction of the potential geographic distribution of the ectomycorrhizal mushroom *Tricholoma matsutake* under multiple climate change scenarios. Sci. Rep. 7, 46221. https://doi.org/10.1038/srep46221.

He, P.F., He, L., Zhang, A.Q., Wang, X.L., Qu, L., Sun, P.L., 2017. Structure and chain conformation of a neutral polysaccharide from sclerotia of *Polyporus umbellatus*. Carbohyd. Polym. 155, 61–67. https://doi.org/10.1016/j.carbpol.2016.08.041.

IPCC, 2013. Climate Change 2013: the physical science basis. Contribution of Working Group I to the fifth assessment report of the Intergovernmental Panel on climate change. Cambridge University Press, New York.

Leathwick, J.R., Elith, J., Hastie, T., 2006. Comparative performance of generalized additive models and multivariate adaptive regression splines for statistical modelling of species distributions. Ecol. Model. 199, 188–196. https://doi.org/10.1016/j.ecolmodel.2006.05.022.

Lenoir, J., Gégout, J.C., Marquet, P.A., De Ruffray, P., Brisse, H., 2008. A significant upward shift in plant species optimum elevation during the 20th century. Science 320, 1768–1771. https://doi.org/10.1126/science.1156831.

Li, W.R., Liang, Z.S., Chen, D.Y., 2012. Research advance in the biological characteristics of *Polyporus umbellatus*. J. Northwest. For. Univ. 27, 60–65 (In Chinese).

Li, X., Tian, H., Wang, Y., Li, R., Song, Z., Zhang, F., Xu, M., Li, D., 2013. Vulnerability of 208 endemic or endangered species in China to the effects of climate change. Reg. Environ. Chang. 13, 843–852. https://doi.org/10.1007/s10113-012-0344-z.

Liu, M.M., Xing, Y.M., Guo, S.X., 2015a. Habitat suitability assessment of medicinal *Polyporus umbellatusin* China based on maxent modeling. Chin. J. Chin. Mater. Med. 40, 2792–2795 (In Chinese).

Liu, M.M., Xing, Y.M., Guo, S.X., 2015b. Diversity analysis of *Polyporus umbellatus* in China using inter-simple sequence repeat (ISSR) markers. Biol. Pharm. Bull. 38, 1512–1517. https://doi.org/10.1248/bpb.b15-00274.

Lu, C.Y., Gu, W., Dai, A.H., Wei, H.Y., 2012. Assessing habitat suitability based on geographic infomation system (GIS) and fuzzy: a case study of *Schisandra sphenanthera* Rehd. Et Wils. in Qinling Mountains, China. Ecol. Model. 242, 105–115.

Marmion, M., Luoto, M., Heikkinen, R.K., Thuiller, W., Gaucherel, C., Houet, T., 2009. The performance of state-of-the-art modelling techniques depends on geographical distribution of species. Ecol. Model. 220, 3512–3520. https://doi.org/10.1016/j.ecolmodel.2008.10.019.

Merow, C., Smith, M.J., Silander, J.A., 2013. A practical guide to MaxEnt for modeling species' distributions: what it does, and why inputs and settings matter. Ecography 36, 1058–1069. https://doi.org/10.1111/j.1600-0587.2013.07872.x.

Mi, C., Huettmann, F., Guo, Y., Han, X., Wen, L., 2017. Why choose random forest to predict rare species distribution with few samples in large undersampled areas? Three Asian crane species models provide supporting evidence. PeerJ 5, e2849. https://doi.org/10.7717/peerj.2849.

Moisen, G.G., Freeman, E.A., Blackard, J.A., Frescino, T.S., Zimmermann Jr., N.E., Edwards, T.C., 2006. Predicting tree species presence and basal area in Utah: a comparison of stochastic gradient boosting, generalized additive models, and tree-based methods. Ecol. Model. 199, 176–187. https://doi.org/10.1016/j.ecolmodel.2006.05.021.

Naimi, B., Araújo, M.B., 2016. sdm: a reproducible and extensible r platform for species distribution modelling. Ecography 39, 368–375. https://doi.org/10.1111/ecog.01881.

Phan, C.W., David, P., Sabaratnam, V., 2017. Edible and medicinal mushrooms: emerging brain food for the mitigation of neurodegenerative diseases. J. Med. Food 20, 1–10. https://doi.org/10.1089/jmf.2016.3740.

Phillips, S.J., Anderson, R.P., Schapire, R.E., 2006. Maximum entropy modeling of species geographic distributions. Ecol. Model. 190, 231–259. https://doi.org/10.1016/j.ecolmodel.2005.03.026.

Song, C., Liu, M., Xing, Y., Guo, S., 2014. ESTs analysis of putative genes engaged in *Polyporus umbellatus* sclerotial development. Int. J. Mol. Sci. 15, 15951–15962. https://doi.org/10.3390/ijms150915951.

Strubbe, D., Jackson, H., Groombridge, J., Matthysen, E., 2015. Invasion success of a global avian invader is explained by within-taxon niche structure and association with humans in the native range. Divers. Distrib. 21, 675–685. https://doi.org/10.1111/ddi.12325.

Summers, D.M., Bryan, B.A., Crossman, N.D., Meyer, W.S., 2012. Species vulnerability to climate change: impacts on spatial conservation priorities and species representation. Glob. Change Biol. 18, 2335–2348. https://doi.org/10.1111/j.1365-2486.2012.02700.x.

Suz, L.M., Barsoum, N., Benham, S., Cheffings, C., Cox, F., Hackett, L., Jones, A.G., Mueller, G.M., Orme, D., Seidling, W., Van Der Linde, S.V.D., Bidartondo, M.I., 2015. Monitoring ectomycorrhizal fungi at large scales for science, forest management, fungal conservation and environmental policy. Ann. For. Sci. 72, 877–885. https://doi.org/10.1007/s13595-014-0447-4.

Thuiller, W., Lafourcade, B., Engler, R., Araújo, M.B., 2009. Biomod – a platform for ensemble forecasting of species distributions. Ecography 32, 369–373. https://doi.org/10.1111/j.1600-0587.2008.05742.x.

Tian, F., 2015. Investigation on *Polyporus umbellatus* Resource. (Master's Thesis). Shaanxi Normal University, Xi'an, China (In Chinese).

Xing, Y.M., Chen, J., Lv, Y.L., Liang, H.Q., Guo, S.X., 2011. Determination of optimal carbon source and pH value fors clerotial formation of *Polyporus umbellatus* under artificial conditions. Mycol. Prog. 10, 121–125. https://doi.org/10.1007/s11557-010-0725-y.

Xing, X., Ma, X., Guo, S., 2012. Fungal species residing in the sclerotia of *Polyporus umbellatus*. Symbiosis 56, 19–24. https://doi.org/10.1007/s13199-012-0155-5.

Xing, X., Ma, X., Hart, M.M., Wang, A., Guo, S., 2013. Genetic diversity and evolution of Chinese traditional medicinal fungus *Polyporus umbellatus* (Polyporales, Basidiomycota). PLoS One 8, e58807. https://doi.org/10.1371/journal.pone.0058807.

Yang, X.Q., Kushwaha, S.P.S., Saran, S., Xu, J., Roy, P.S., 2013. Maxent modeling for predicting the potential distribution of medicinal plant, *Justicia adhatoda*, L. in lesser himalayan foothills. Ecol. Eng. 51, 83–87.

Yuan, H.S., Wei, Y.L., Wang, X.G., 2015. Maxent modeling for predicting the potential distribution of sanghuang, an important group of medicinal fungi in China. Fungal Ecol. 17, 140–145. https://doi.org/10.1016/j.funeco.2015.06.001.

Zhang, T., 2014. The Trend of *Polyporus umbellatus* Industry and Development Research Report. (Master's Thesis). Northwest Agriculture and Forestry University (In Chinese).

Zhao, Y.Y., 2013. Traditional uses, phytochemistry, pharmacology, pharmacokinetics and quality control of *Polyporus umbellatus* (pers.) fries: a review. J. Ethnopharmacol. 149, 35–48. https://doi.org/10.1016/j.jep.2013.06.031.

Zhao, Z.Z., Guo, Y.L., Wei, H.Y., Ran, Q., Gu, W., 2017. Predictions of the potential geographical distribution and quality of a *Gynostemma pentaphyllum* base on the fuzzy matter element model in China. Sustainability 9, 1114. https://doi.org/10.3390/su9071114.

Zimmermann, N.E., Edwards, T.C., Graham, C.H., Pearman, P.B., Svenning, J., 2010. New trends in species distribution modelling. Ecography 33, 985–989. https://doi.org/10.1111/j.1600-0587.2010.06953.x.